



Contents lists available at ScienceDirect

Quaternary Science Reviews

journal homepage: www.elsevier.com/locate/quascirev

Noble gases in the sediments of Lake Van – solute transport and palaeoenvironmental reconstruction

Yama Tomonaga^{a, *}, Matthias S. Brennwald^a, Ayşegül F. Meydan^b, Rolf Kipfer^{a, c, d}^a Eawag, Swiss Federal Institute of Aquatic Science and Technology, Water Resources and Drinking Water, Duebendorf, Switzerland^b Department of Geological Engineering, Yuzuncu Yil University, Van, Turkey^c Institute of Biogeochemistry and Pollutant Dynamics, Swiss Federal Institute of Technology, Zurich, Switzerland^d Institute of Geochemistry and Petrology, Swiss Federal Institute of Technology, Zurich, Switzerland

ARTICLE INFO

Article history:

Received 20 August 2013

Received in revised form

3 September 2014

Accepted 5 September 2014

Available online xxx

Keywords:

ICDP

PaleoVan

Deep drilling

Terrestrial He emission

Palaeosalinity

ABSTRACT

Sediment samples acquired in 2010 from the long cores of the International Continental Scientific Drilling Program (ICDP) PaleoVan drilling project on Lake Van for noble-gas analysis in the pore water allow determination of the local terrestrial He-gradient as a function of depth within a sediment column of more than 200 m. These measurements yield first insights into the physical transport mechanisms of terrigenous He through the uppermost part of unconsolidated lacustrine sediments overlying the continental crust.

In line with our previous work on the spatial distribution of the terrigenous He release into Lake Van, we identify a high He concentration gradient in the uppermost 10 m of the sediment column. The He concentration gradient decreases below this depth down to approx. 160 m following in general the expectations of the modelling of radiogenic He production and transport in a sediment column with homogeneous fluid transport properties. Overall the in-situ radiogenic He production due to the decay of U and Th in the mineral phases of the sediments accounts for about 80% of the He accumulation. At approx. 190 m we observe a very high He concentration immediately below a large lithological unit characterised by strong deformations. We speculate that this local enrichment is the result of the lower effective diffusivities in the pore space that relate to the abrupt depositional history of this deformed unit. This particular lithological unit seems to act as a barrier that limits the transport of solutes in the pore space and hence might “trap” information on the past geochemical conditions in the pore water of Lake Van.

The dissolved concentrations of atmospheric noble gases in the pore waters of the ICDP PaleoVan cores are used to geochemically reconstruct salinity on the time scale of 0–55 ka BP. Higher salinities in the pore water at a depth of about 20 m suggest a significantly lower lake level of Lake Van in the past.

© 2014 Elsevier Ltd. All rights reserved.

1. Introduction

In the last few decades, noble gases in aquatic systems have become a well-established geochemical tool for investigating physical transport and exchange processes in lakes, oceans, and ground waters and for reconstructing past climate conditions (for reviews see Kipfer et al., 2002; Schlosser and Winckler, 2002; Aeschbach-Hertig and Solomon, 2013; Brennwald et al., 2013; Stanley and Jenkins, 2013).

The varved sediments of Lake Van have been identified as an important palaeoclimate archive, storing information on the past environmental conditions prevailing in eastern Anatolia. Therefore, the sediments of Lake Van have been targeted by a deep-drilling project of the International Continental Scientific Drilling Program (ICDP, www.icdp-online.org) to reconstruct the glacial and interglacial cycles during the last 600 ka (Litt et al., 2009, 2011, 2014; Baumgarten et al., 2014; Çağatay et al., 2014; Cukur et al., 2014a, 2014b; Kwiczen et al., 2014; Litt and Anselmetti, 2014; Randlett et al., 2014; Stockhecke et al., 2014a, 2014b; Vigliotti et al., 2014). In 2010 the ICDP drilling project PaleoVan recovered sediment cores of up to 220 m in length with the aim of studying this unique high-resolution sedimentological archive not only in terms of palaeoclimatic reconstruction, but also to constrain

* Corresponding author. Eawag, Ueberlandstrasse 133, CH-8600 Duebendorf, Switzerland. Tel.: +41 58 765 5365.

E-mail address: tomonaga@eawag.ch (Y. Tomonaga).

terrigenous fluid transport processes in the deep sediment column using noble gases (Litt et al., 2009, 2012), as Lake Van is known to accumulate terrigenous He enriched in ^3He from a mantle source (e.g., Kipfer et al., 1994).

In this work we present He, Ne, Ar, Kr, and Xe concentrations as well as the $^3\text{He}/^4\text{He}$, $^{20}\text{Ne}/^{22}\text{Ne}$, and $^{36}\text{Ar}/^{40}\text{Ar}$ isotope ratios measured in sediment pore water samples of Lake Van acquired during the drilling operations of the ICDP PaleoVan project at Ahlat Ridge (Fig. 1; Litt et al., 2009, 2011, 2012). Our previous research on the mixing dynamics and on the He emanation in Lake Van (Kipfer et al., 1994; Kaden et al., 2010; Tomonaga et al., 2011a), as well as the newly parameterised noble-gas solubility equations for its alkaline water (Tomonaga et al., 2012), set the basis for our evaluations. He concentrations are discussed in terms of fluid transport properties of the sediment column and terrigenous He emission from the solid earth. Atmospheric noble gases are interpreted, whenever possible, in terms of past environmental and hydrochemical conditions in Lake Van.

1.1. He and the fluid transport in the pore space

Terrigenous He is known to emanate from the solid earth into the atmosphere (see e.g., O’Nions and Oxburgh, 1983; Mamyurin and Tolstikhin, 1984; Ballentine et al., 2002). Pore waters of unconsolidated sediments in lakes and in the oceans represent an ideal geochemical environment for assessing the local He emission, thus allowing fluid transport in the uppermost part of the Earth’s crust to be studied (Chaduteau et al., 2009; Lan et al., 2010; Tomonaga et al., 2011a, 2013). The transport of He within the sediment column can be described by advection and diffusion, where He

migrates through the connected pore space of an unconsolidated sediment column (e.g., Berner, 1975; Imboden, 1975; Strassmann et al., 2005). In contrast to the open water body, the pore water in lacustrine and oceanic sediments records the spatial variability of the He emission. The pore waters of unconsolidated sediments are therefore a suitable system to analyse the rates and the spatial variability of He transport and release (Brennwald et al., 2013).

By analysing the pore water in the uppermost 2 m of the sediments of Lake Van, Tomonaga et al. (2011a) determined a terrigenous $^3\text{He}/^4\text{He}$ isotope ratio range of $(2.5\text{--}4.1) \cdot 10^{-6}$ suggesting that the He entering the lake is a mixture of mantle He and radiogenic He being produced in the sediment column or in the rock basement. The study also mapped the spatial distribution of the He emission at the sediment–water interface of Lake Van and identified three characteristic He concentration gradients being associated with three characteristic He fluxes (Fig. 1, for details see Tomonaga et al., 2011a): low flux (“L” cores: $(0.4\text{--}0.8) \cdot 10^8$ atoms/m²/s), high flux (“H” cores: $(2\text{--}5) \cdot 10^8$ atoms/m²/s), and “hot spot” flux (“S” cores: $(18\text{--}42) \cdot 10^8$ atoms/m²/s). The highest fluxes have been identified not in the centre, but at the steep borders of the main deep basin of Lake Van (the Tatvan basin, see Fig. 1).

1.2. Atmospheric noble gases to reconstruct past environmental conditions

The equilibrium partitioning of noble gases between air and water can be approximated reasonably by Henry’s Law (Ozima and Podosek, 1983; Kipfer et al., 2002; Brennwald et al., 2013). As the Henry coefficients depend mainly on the temperature and on the salinity of the water mass involved in the gas exchange, the

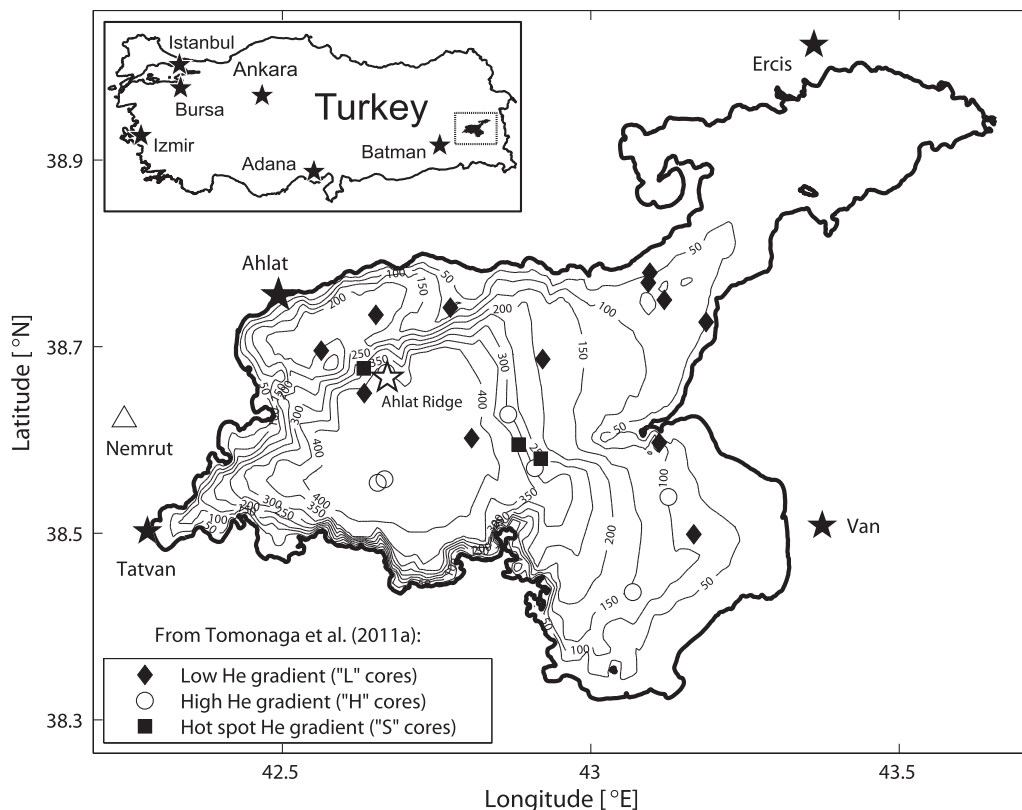


Fig. 1. Location of Lake Van (Turkey) and the main ICDP PaleoVan drill site at Ahlat Ridge (empty star) together with the position of low (“L” cores, black diamonds), high (“H” cores, empty circles), and hot spot (“S” cores, black squares) He concentration gradients determined in the pore water of short sediment cores (Tomonaga et al., 2011a). Major cities are represented by black stars. The triangle indicates the position of the Nemrut volcano (the most active volcano in the study area).

equilibrium concentrations of noble gases dissolved in the water directly reflect the physical conditions that prevailed when the water was last in contact with the atmosphere.

During sedimentation, water from the sediment–water interface is incorporated into the pore space of the growing sediment column. The concentrations of atmospheric noble gases in the pore water are, therefore, expected to match the noble-gas concentrations of the overlying water mass at the time when the sediment was deposited (Brennwald et al., 2013). Concentration signals in the pore water are expected to be smoothed over time by diffusive transport. However, on depth scales of about 1–10 m or more and according to the specific effective diffusivity characterizing the pore space, such signals can be preserved over time scales of a few millennia or more (Brennwald et al., 2004, 2005, 2013; Strassmann et al., 2005) and thus be detected in a sedimentary record.

The effective diffusivity in the uppermost few metres of the sediments of Lake Van was shown to be only about 10–20% of the molecular diffusion coefficient in bulk water (Tomonaga et al., 2011a). Such attenuation of the diffusive transport in the pore space indicates that the sediments of Lake Van are potentially able to preserve dissolved concentration signals resulting from environmental changes in the past (Brennwald et al., 2003, 2005, 2013; Strassmann et al., 2005; Kwiecien et al., 2012; Randlett et al., 2014).

As an endorheic water body Lake Van reacts very sensitively to environmental changes. Changes in the precipitation regime, for instance, induce significant lake level fluctuations (Kadioglu et al., 1997; Kiliñçaslan, 2000; Kaden et al., 2010). The mixing dynamics of Lake Van in response to lake level fluctuations (i.e., inducing changes in the water temperature and salinity and, thus, also in the dissolved noble-gas concentrations; Kaden et al., 2010) underline the potential of its sediments as a climatic and environmental archive (Litt et al., 2009, 2011, 2012).

2. Regional setting

Lake Van, the largest soda lake on earth, is located in a tectonically active region of eastern Anatolia (Turkey) at about 1650 m above the sea level (Fig. 1). This region is situated in the vicinity of the triple junction of the Eurasian, Afro-Arabian and Persian plates. Such a tectonic setting favours the emission of fluids from the deep lithosphere into the lake basin and Lake Van is known to accumulate mantle He (Kipfer et al., 1994; Kaden et al., 2010; Tomonaga et al., 2011a).

The geology of the northern part of the basin is dominated by volcanic rocks whereas in the southern part the intrusive and metamorphic rocks of the Bitlis massif prevail (Keskin, 2007; Cukur et al., 2012).

Lake Van is one of the largest terminal lakes on earth, which, in combination with the volcanic environment (e.g., Sumita and Schmincke, 2013a, 2013b), explains its high salinity (23 g/kg; e.g., Kempe et al., 1991; Tomonaga et al., 2012) and high pH (approx. 10; Kempe et al., 1991).

The sedimentary sequence collected by the ICDP PaleoVan project consists of approx. 76% lacustrine carbonaceous clayey silt, approx. 2% fluvial deposits, approx. 17% volcanoclastic deposits and approx. 5% gaps (for details see Stockhecke et al., 2014a).

3. Material and methods

3.1. Noble-gas sampling and analysis

The samples for noble-gas analysis were acquired on the Deep Lake Drilling System managed by DOSECC (Drilling, Observation and Sampling of the Earth's Continental Crust; <http://www.dosecc.org>) during the ICDP PaleoVan drilling operations in 2010 by

adapting our standard technique to sample noble gases in unconsolidated sediments (Brennwald et al., 2003). We only sampled sediment sections that were not severely affected by macroscopic bubble formation in order to prevent degassing artefacts. However, we cannot fully exclude that gas loss occurred during the sampling (see Section 4.1).

Immediately after core recovery on the platform, the bulk sediment was transferred into small copper tubes (inner diameter approx. 6 mm, length approx. 60 cm) by squeezing the sediment core with an aluminium piston moving along the axis of the plastic liner. To transfer the bulk sediment into the copper tubes we developed a full-metal sediment squeezer in order to apply by a hydraulic press the needed 8 tons of force on the piston located at the bottom of the liner. To avoid deformation of the liner during squeezing, the plastic liner was supported by an external aluminium tube (wall thickness of about 6 mm). The copper tubes, which were attached to the top of the liner using a steel cover and Swagelok fittings, were filled with bulk sediment and sealed airtight by closing two metal clamps (Beyerle et al., 2000; Tomonaga et al., 2011b; Brennwald et al., 2003, 2013). The steel cover was fitted with a steel tube of the same inner and outer diameters as the copper tubes. This tube penetrates about 5 cm into the sediments and acts as a port for the transferred sediment in order to minimise air contamination and degassing that may occur at the sediment surface (see Brennwald et al., 2003, 2013; Chaduteau et al., 2007; Tomonaga et al., 2011b).

Sample preparation in the laboratory was carried out according to the method of Tomonaga et al. (2011b). The copper tube containing each sample was divided into two aliquots (i.e., two 9.5-cm-long copper tubes) by placing four additional metal clamps. Each aliquot was then centrifuged to separate the pore water from the sediment matrix.

Adaptations to the geometrical arrangement were needed to fit the closed copper tubes into a high-speed centrifuge with a fixed-angle rotor (Herolab HiCen XL with an A6.9 rotor; Tomonaga et al., 2013). The aluminium fittings necessary to hold and support the sampling containers were designed to correspond to the inner dimensions of the standard 500 mL polypropylene centrifuging bottles. For centrifuging, each sample with its supporting fittings was inserted into one of the polypropylene bottles. The bottles act as a protection for the rotor and allow the weight of each sample to be adjusted easily with water to avoid rotor imbalance. Prior to centrifuging, the samples were put in an ultrasonic bath for about 30 min to loosen the bulk sediment matrix from the copper tube wall. Then the samples were centrifuged for 4 h at 9000 rpm and again placed in the ultrasonic bath. The samples were then centrifuged a second time for 4 h at 3600 rpm using an AS 4.1000 swing-out rotor with four 1000 mL buckets in the same centrifuge. The fittings to hold the samples in the buckets of the swing-out rotor were made of polypropylene to avoid weight overload and were geometrically adapted to the standard 1000 mL PPCO bottles (Herolab Item 253572).

The second ultrasonic bath treatment and the subsequent second centrifuging are needed to orientate the sediment–water interface perpendicular to the axis of the copper tube, as only such a configuration enables the adequate final mounting of the third clamp which separates the pure water from the sediment matrix phase.

After the centrifuging process, one aliquot was pinched off at a position located slightly above the sediment–water interface, which was determined by visual inspection by opening the copper tube of the other aliquot (Tomonaga et al., 2011b).

Noble-gas analysis was conducted only on the separated pore water according to the well-established experimental protocols commonly used to determine noble-gas abundances in water samples (Beyerle et al., 2000).

For some samples from deep core sections the centrifuging process only separated very low amounts of pore water (<1 g). Acknowledging the geometrical constraints of the current experimental setup, these samples were pinched off as close as possible to the top clamp. In these samples the complete separation of pore water and sediment matrix cannot be guaranteed. Such incomplete separation may result in the incomplete extraction of noble gases trapped in sediment clusters that might remain in the water side of the copper tubes. However, even an incomplete extraction is not expected to considerably bias of the He results, as He extraction from such sediment chunks has been shown (in contrast to the heavier noble gases) to be sufficiently complete (Tomonaga et al., 2013).

3.2. Noble-gas temperatures (NGTs) and salinities (NGSs)

Noble-gas concentrations in the water body of Lake Van do not agree well with the noble-gas concentrations in air-saturated water (ASW) calculated using existing solubility parameterisations (Tomonaga et al., 2012). Thus, we proposed empirical salinity factors accounting for the specific hydrochemistry of Lake Van to correctly calculate the ASW concentrations (Tomonaga et al., 2012). These salinity factors allow consistent reconstruction of past physical conditions (i.e., NGTs and NGSs) in the lake by converting the measured concentrations (i.e., concentrations related to the soda chemistry of the water of Lake Van) into “seawater-like” concentrations. Such converted noble gas concentrations can be used in existing fitting procedures (accounting for noble gas solubility equations in seawater or NaCl solutions; e.g., Aeschbach-Hertig et al., 1999; Ballentine and Hall, 1999) to determine NGTs and NGSs.

In this work we used the closed-system equilibration (CE) model (for a recent review see Aeschbach-Hertig and Solomon, 2013) to reconstruct NGs in Lake Van.

4. Results and discussion

Table 1 lists the results of the noble-gas measurements in the ICDP PaleoVan sediment samples together with the respective overall analytical 1- σ errors.

4.1. Degassing and He concentration correction

Significant gas loss (“degassing”) is observed below 25 m, as indicated by the lower noble-gas concentrations determined in the deep sediments with respect to the concentrations measured close to sediment–water interface (e.g., at 0.44 m and 0.59 m) and in the water immediately above the sediment–water interface (Table 1, sample at 0 m). The observed gas loss can conceptually be modelled as the result of gas equilibration between pore water and gas bubbles and accordingly corrected if the reasonable assumption is made that prior to degassing the concentrations of the purely atmospheric noble gases in the sediment pore water (Ne, Ar, Kr, Xe) agreed with the ASW concentrations resulting from air/water equilibration at the lake surface (Brennwald et al., 2005).

For five samples the $^{20}\text{Ne}/^{22}\text{Ne}$ or $^{36}\text{Ar}/^{40}\text{Ar}$ values are higher (considering the 1- σ error level) than the isotope ratios of air or ASW (Fig. 2). We note that such fractionation pattern cannot be explained by degassing as such process tends to deplete the light noble gas isotopes in the pore water phase. The observed enrichment of light noble gas isotopes might conceptually result from an

Table 1
Noble-gas concentrations, noble-gas isotope ratios, corrected He concentrations, and the respective uncertainties (at the 1- σ level) measured in the ICDP PaleoVan sediment samples. 1 cm³ STP = 22414⁻¹ mol.

Sample	Section	Depth (m)	He (10 ⁻⁸ cm ³ STP/g)	Ne (10 ⁻⁷ cm ³ STP/g)	Ar (10 ⁻⁴ cm ³ STP/g)	Kr (10 ⁻⁸ cm ³ STP/g)	Xe (10 ⁻⁸ cm ³ STP/g)	³ He/ ⁴ He (10 ⁻⁶)	²⁰ Ne/ ²² Ne	³⁶ Ar/ ⁴⁰ Ar (10 ⁻³)	He (corrected) (10 ⁻⁸ cm ³ STP/g)
wa,405,2797	Sed/water interface	0.00	4.48 ± 0.02	1.57 ± 0.02	3.06 ± 0.01	7.27 ± 0.04	1.09 ± 0.01	2.87 ± 0.03	9.80 ± 0.01	3.379 ± 0.001	4.5 ± 0.1
se,405,2798	5034_2_Z_1_1	0.44	6.5 ± 0.1	2.07 ± 0.03	3.43 ± 0.04	7.8 ± 0.1	1.15 ± 0.02	2.73 ± 0.08	9.94 ± 0.07	3.368 ± 0.005	6 ± 1
se,405,2799	5034_2_Z_1_1	0.59	5.50 ± 0.08	1.75 ± 0.03	3.14 ± 0.04	7.4 ± 0.1	1.09 ± 0.02	2.48 ± 0.07	9.6 ± 0.1	3.38 ± 0.01	5.5 ± 0.4
se,405,2840	5034_2_D_2_3	4.56	13.8 ± 0.4	1.52 ± 0.05	2.94 ± 0.09	7.0 ± 0.2	1.09 ± 0.03	2.25 ± 0.06	9.7 ± 0.3	3.38 ± 0.05	14 ± 1
se,422,2840	5034_2_D_2_3	4.56	16.42 ± 0.08	1.71 ± 0.02	2.99 ± 0.01	6.89 ± 0.05	1.06 ± 0.03	2.59 ± 0.03	9.7 ± 0.1	3.36 ± 0.03	16 ± 2
se,422,2824	5034_2_E_4_1	10.92	20.4 ± 0.1	2.37 ± 0.02	3.27 ± 0.01	6.95 ± 0.05	1.03 ± 0.03	2.58 ± 0.02	9.5 ± 0.2	3.38 ± 0.02	20 ± 6
se,422,2844	5034_2_D_6_4	19.77	23.1 ± 0.1	1.15 ± 0.01	2.483 ± 0.005	6.23 ± 0.05	1.02 ± 0.03	2.89 ± 0.03	9.3 ± 0.2	3.37 ± 0.02	23.1 ± 0.5
se,422,2822	5034_2_E_8_2	24.11	22.9 ± 0.1	0.90 ± 0.01	2.208 ± 0.004	5.72 ± 0.05	1.01 ± 0.02	3.11 ± 0.04	9.3 ± 0.4	3.39 ± 0.08	60 ± 8
se,422,2841	5034_2_D_10_1	29.16	6.92 ± 0.08	0.43 ± 0.01	1.334 ± 0.002	3.93 ± 0.03	0.88 ± 0.02	2.77 ± 0.07	9.7 ± 0.4	3.39 ± 0.05	40 ± 17
se,422,2851	5034_2_E_11_3	34.56	2.17 ± 0.08	0.24 ± 0.00	0.824 ± 0.002	1.79 ± 0.03	0.57 ± 0.01	1.9 ± 0.1	7.6 ± 0.7	3.38 ± 0.02	36 ± 24
se,422,2814	5034_2_E_13_2	38.45	0.85 ± 0.06	0.04 ± 0.00	0.1997 ± 0.0004	1.20 ± 0.01	0.50 ± 0.01	2.6 ± 0.1	6 ± 3	3.2 ± 0.5	24 ± 19
se,420,2850	5034_2_D_17_3	50.54	0.45 ± 0.09	0.06 ± 0.00	0.25 ± 0.01	1.19 ± 0.05	0.38 ± 0.02	3.6 ± 0.8	9 ± 3	3.2 ± 0.2	19 ± 16
se,422,2845	5034_2_E_18_1	53.61	2.35 ± 0.09	0.17 ± 0.01	0.365 ± 0.002	0.86 ± 0.01	0.25 ± 0.01	1.7 ± 0.1	12 ± 2	3.6 ± 0.1	148 ± 127
se,422,2810	5034_2_D_20_3	58.75	6.97 ± 0.06	1.61 ± 0.02	0.872 ± 0.002	1.89 ± 0.03	0.45 ± 0.01	1.52 ± 0.04	9.9 ± 0.2	3.33 ± 0.08	159 ± 82
se,422,2806	5034_2_E_21_1	62.75	2.30 ± 0.08	0.25 ± 0.00	0.365 ± 0.001	1.32 ± 0.01	0.40 ± 0.01	2.28 ± 0.09	7.6 ± 0.9	3.5 ± 0.4	89 ± 71
se,422,2808	5034_2_E_23_1	68.84	2.40 ± 0.06	0.43 ± 0.01	0.563 ± 0.001	1.60 ± 0.02	0.46 ± 0.01	2.15 ± 0.07	8.8 ± 0.6	3.5 ± 0.2	69 ± 51
se,422,2838	5034_2_D_26_5	71.46	1.04 ± 0.08	0.14 ± 0.01	0.2392 ± 0.0005	1.14 ± 0.02	0.46 ± 0.01	2.0 ± 0.2	6.9 ± 0.8	3.6 ± 0.2	37 ± 30
se,422,2849	5034_2_D_28_3	77.08	2.66 ± 0.09	0.55 ± 0.01	0.787 ± 0.001	2.40 ± 0.03	0.61 ± 0.02	1.78 ± 0.08	10.0 ± 0.5	3.4 ± 0.1	42 ± 27
se,422,2826	5034_2_E_32_1	96.28	0.78 ± 0.04	0.10 ± 0.00	0.176 ± 0.001	0.57 ± 0.02	0.17 ± 0.01	2.1 ± 0.1	5.6 ± 0.9	3.4 ± 0.2	79 ± 72
se,420,2848	5034_2_D_38_3	107.98	6.6 ± 0.2	1.85 ± 0.05	1.12 ± 0.03	2.00 ± 0.06	0.32 ± 0.02	1.5 ± 0.1	9.7 ± 0.2	3.33 ± 0.05	153 ± 72
se,422,2832	5034_2_F_4_2	112.10	2.12 ± 0.03	0.33 ± 0.00	0.388 ± 0.001	1.14 ± 0.02	0.33 ± 0.01	2.58 ± 0.08	9.5 ± 0.7	3.5 ± 0.3	90 ± 72
se,422,2831	5034_2_F_5_3	116.38	1.0 ± 0.1	0.14 ± 0.01	0.260 ± 0.001	0.98 ± 0.02	0.31 ± 0.01	1.8 ± 0.1	6.4 ± 0.8	3.1 ± 0.2	50 ± 43
se,422,2830	5034_2_G_6_1	132.86	4.51 ± 0.06	0.93 ± 0.01	0.600 ± 0.001	1.32 ± 0.01	0.41 ± 0.01	1.71 ± 0.07	9.8 ± 0.3	3.31 ± 0.09	111 ± 74
se,422,2837	5034_2_G_7_1	135.91	3.61 ± 0.05	0.75 ± 0.01	0.603 ± 0.001	1.45 ± 0.02	0.39 ± 0.01	2.09 ± 0.08	9.3 ± 0.4	3.6 ± 0.1	84 ± 58
se,422,2857	5034_2_G_9_1	142.00	4.9 ± 0.4	0.76 ± 0.01	0.503 ± 0.001	1.06 ± 0.02	0.23 ± 0.01	1.90 ± 0.06	9.4 ± 0.4	3.4 ± 0.1	174 ± 129
se,420,2855	5034_2_G_11_2	149.16	13.0 ± 0.4	2.50 ± 0.07	1.68 ± 0.05	2.78 ± 0.08	0.35 ± 0.01	2.6 ± 0.1	9.7 ± 0.1	3.38 ± 0.05	149 ± 40
se,422,2800	5034_2_F_13_2	152.09	11.18 ± 0.08	3.26 ± 0.03	1.919 ± 0.004	2.57 ± 0.03	0.31 ± 0.01	1.73 ± 0.05	9.37 ± 0.06	3.35 ± 0.05	128 ± 19
se,422,2829	5034_2_G_12_3	153.29	3.3 ± 0.1	0.40 ± 0.01	0.365 ± 0.001	1.02 ± 0.02	0.33 ± 0.01	3.4 ± 0.1	8.6 ± 0.7	3.6 ± 0.3	137 ± 109
se,422,2836	5034_2_G_14_1	157.25	1.5 ± 0.1	0.07 ± 0.01	0.098 ± 0.001	0.44 ± 0.02	0.15 ± 0.01	3.4 ± 0.2	8 ± 3	3 ± 1	192 ± 179
se,422,2827	5034_2_G_24_2	181.98	3.27 ± 0.08	0.30 ± 0.01	0.284 ± 0.001	0.84 ± 0.02	0.27 ± 0.01	2.96 ± 0.09	8.8 ± 0.9	3.9 ± 0.4	191 ± 160
se,422,2843	5034_2_G_27_3	189.37	65.7 ± 0.3	1.02 ± 0.01	0.753 ± 0.002	1.41 ± 0.02	0.40 ± 0.01	4.05 ± 0.02	9.8 ± 0.3	3.1 ± 0.1	1703 ± 1094
se,420,2846	5034_2_G_30_3	197.99	6.8 ± 0.2	0.35 ± 0.01	0.48 ± 0.01	1.41 ± 0.04	0.39 ± 0.02	3.3 ± 0.2	7.6 ± 0.7	3.50 ± 0.08	230 ± 177
se,422,2839	5034_2_G_32_4	205.47	10.2 ± 0.1	0.25 ± 0.00	0.391 ± 0.001	1.00 ± 0.02	0.24 ± 0.01	3.69 ± 0.03	8.0 ± 0.8	3.1 ± 0.2	627 ± 527

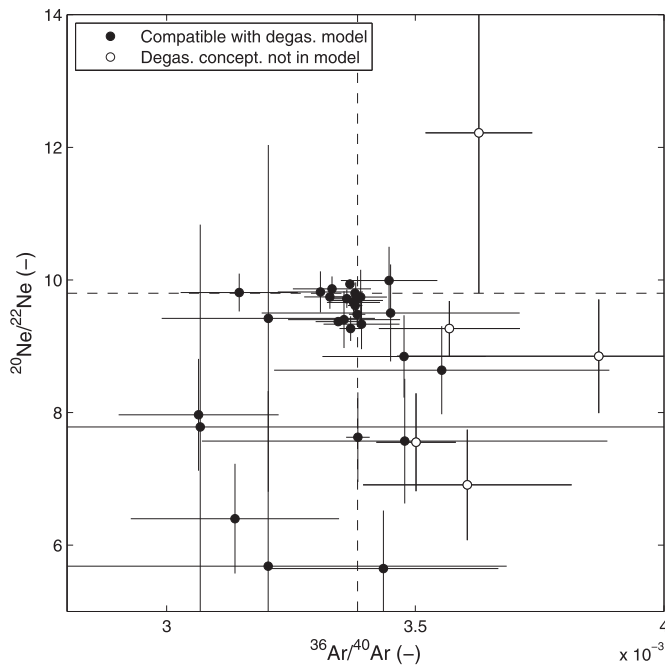


Fig. 2. $^{36}\text{Ar}/^{40}\text{Ar}$ ratios plotted against the $^{20}\text{Ne}/^{22}\text{Ne}$ ratios (uncertainties at the $1-\sigma$ error level). The dashed lines represent the ASW ratios. Empty dots indicate samples enriched in light Ne and Ar isotopes that might be affected by secondary gas exchange (i.e., gas exchange occurred after the inclusion of the pore water into the sediments; see Section 4.1) with a free gas phase. The black dots represent samples that agree with the expected values for air-saturated water or can be understood as analytical “outliers” within the expected statistical discrimination.

in-situ gas exchange between the sediment pore water and a free gas phase. The existence of free gas phases in the sediments of Lake Van has been recently documented by high-resolution seismic data (Cukur et al., 2013). During the formation of such free gas phases (e.g., biogenic methane production) light noble gas isotopes are likely to be stripped from the pore water into the gas phase. Therefore, a correction for degassing considering gas equilibration (i.e., not considering isotope fractionation) between a pore water phase and a free gas phase might not be the most appropriate for these samples (Fig. 3). Due to the elusive nature of the respective fractionation processes, the results from these samples should be interpreted – if at all – only within the broader context of all the noble-gas data obtained from Ahlat Ridge.

Few samples show the $^{20}\text{Ne}/^{22}\text{Ne}$ and $^{36}\text{Ar}/^{40}\text{Ar}$ ratios being lower than the ASW values (Fig. 2). On the $1-\sigma$ error level about one third of the 26 measured samples are expected to show $^{20}\text{Ne}/^{22}\text{Ne}$ or $^{36}\text{Ar}/^{40}\text{Ar}$ ratios not agreeing with the anticipated ASW ratios. Therefore the Ne and Ar isotope ratios of these samples might lie outside the expected statistical $1-\sigma$ range. However, the lower isotope ratios could also indicate diffusion-controlled degassing rather than gas partitioning at equilibrium. Tyroller et al. (2014) showed experimentally that diffusion-controlled isotope fractionation affects Ne much less than Ar (i.e., the determined ratios of the respective diffusion coefficients are $D_{20\text{Ne}}/D_{22\text{Ne}} = 1.010 \pm 0.003$ and $D_{36\text{Ar}}/D_{40\text{Ar}} = 1.055 \pm 0.004$). Diffusion-controlled degassing should result in $^{20}\text{Ne}/^{22}\text{Ne}$ ratios less depleted than the $^{36}\text{Ar}/^{40}\text{Ar}$ ratios with respect to the ASW values. However, the observed extent of fractionation of the Ne isotopes in the samples with low $^{20}\text{Ne}/^{22}\text{Ne}$ ratios is greater than the one for the Ar isotopes, whereby most of the $^{36}\text{Ar}/^{40}\text{Ar}$ ratios agree with the ASW ratio within the $1-\sigma$ error level (Fig. 2). Hence, diffusive gas-exchange does not seem to be the main process leading to the observed lower isotope ratios. Although we cannot completely exclude that

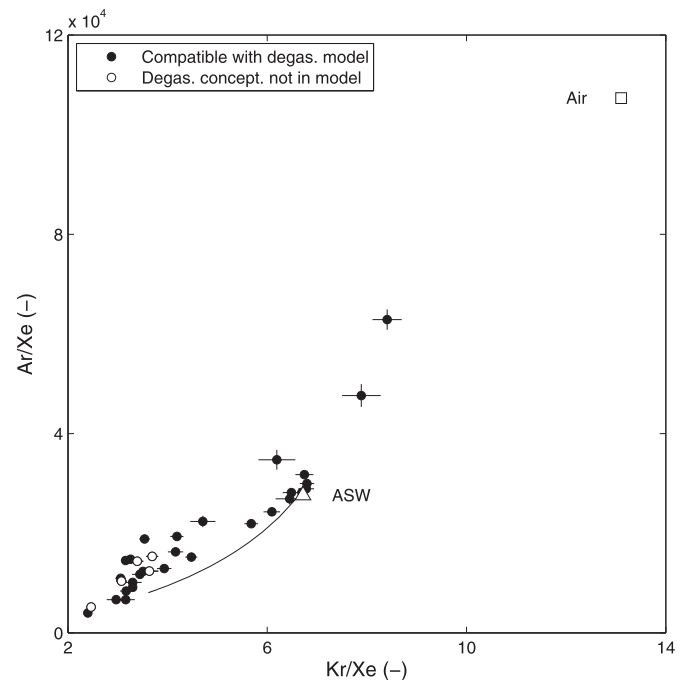


Fig. 3. Three-isotope diagram of the measured Kr/Xe ratios against the Ar/Xe ratios (empty and black dots have the same meaning as in Fig. 2) together with the ratios parameterised by the 1-step-degassing model (solid line; Brennwald et al., 2005) used to correct the measured He concentrations for degassing (Table 1). Although a few samples deviate from the expected values, the model seems to reproduce rather well the observed degassing.

much more complex degassing processes are responsible for the lower Ne and Ar isotope ratios (which can be hardly quantified using the available physical degassing models), we are tempted to classify these isotope ratios as analytical “outliers”.

For the majority of the samples, the $^{20}\text{Ne}/^{22}\text{Ne}$ and $^{36}\text{Ar}/^{40}\text{Ar}$ ratios agree or are very close to the ASW values. As diffusion-controlled Ne and Ar isotope fractionation is not evident, the observed noble-gas depletion can conceptually be understood in terms of loss of a gas phase being equilibrated with the surrounding pore water phase.

Such gas loss can be corrected as described for the case of organic-rich lacustrine sediments in Soppensee using a 1-step-degassing model (Brennwald et al., 2005). The 1-step-degassing model calculates the noble-gas concentration in the pore water after equilibration with a gas phase as $C_i = C_i^*/(1 + B \cdot H_i/P_0)$ using the expected atmospheric equilibrium concentration C_i^* (with $i = \text{Ne, Ar, Kr, Xe}$), the STP bubble volume per unit mass of pore water B , the Henry coefficient H_i for noble gas i (corrected for the specific hydrochemistry of Lake Van, see Section 3.2), and the STP dry-gas pressure P_0 .

We based our degassing correction on Ne, Ar, Kr, and Xe. We estimated B (i.e., the variable parameterising gas loss) for each sample by least-square fitting of the concentrations predicted by the degassing model to the measured noble gas concentrations (Fig. 3; for further details see Brennwald et al., 2005). The error for B is calculated from the deviations of the modelled concentrations with respect to the measured concentrations. The estimation of B is used to calculate the original He concentration in the pore water (i.e., prior to equilibration with the gas phase).

In Fig. 3 two samples (collected at a sediment depth of 149 m and 152 m) lie between the elemental ratios for ASW and air. This might indicate a slight air contamination which, however, cannot be confirmed from the measured He concentrations and isotope

ratios being in agreement with the concentration and isotope ratio ranges of the overlying samples.

The degassing parameterisation yields a corrected He concentration profile that, in accordance with the general expectations (see O’Nions and Oxburgh, 1983, 1988; Oxburgh and O’Nions, 1987; Ballentine et al., 2002) monotonously increases with increasing sediment depth (Fig. 4, black and empty dots) which in turn supports the adequateness of the applied correction.

It should be noted that the applied correction for degassing is a rough approximation that represents a “best guess” which sets the data basis for our interpretations of the He transport within the deep-sediment column of Lake Van. We take into account some of this uncertainty by considering the data errors and their propagation in the calculation of the degassing correction using the 1-step-degassing model (Brennwald et al., 2005).

4.2. Origin of terrigenous He

The ^4He production and release from the minerals of the sediment matrix into the pore water can be roughly estimated from the U and Th concentration profiles determined by downhole logging techniques detecting the specific gamma-radiation (Baumgarten et al., 2014). Gamma ray logging at the Ahlat Ridge drill site over the entire core depth yields the mean U ($C_U = 3.2 \pm 1.4$ ppm) and Th ($C_{Th} = 7.0 \pm 3.7$ ppm) concentrations in the sediments. Assuming a sediment matrix density of 2.5 g/cm^3 and a porosity of 60% (Tomonaga et al., 2011a) the mean ^4He in-situ production rate ($P_{\text{He-4}}$) can be determined from the mean U and Th concentrations ($P_{\text{He-4}} = 0.2355 \cdot 10^{-12} \cdot C_U \cdot [1 + 0.123 \cdot (C_{Th}/C_U - 4)] \text{ (cm}^3\text{STP/g/a)}$); for details on the parameterisation see Zartman et al., 1961; Craig

and Lupton, 1976). $P_{\text{He-4}}$ in the sediment column of Lake Van equals $(9.8 \pm 4.6) \cdot 10^{-13} \text{ cm}^3\text{STP/g/a}$ whereby the error accounts for the standard deviation of the U and Th concentrations.

The error range of the ^4He production rate is rather large in order to cover the major uncertainties that arise from our assumptions. The chosen porosity and matrix density are likely to change with increasing sediment depth and in presence of different lithologies. A porosity of 50% would result in a ^4He production rate close to the upper error limit of $P_{\text{He-4}}$. Such a strong sediment compaction, however, is not likely to affect the investigated sedimentary record. Assuming an unreasonably low density of the sediment matrix (1.4 g/cm^3) does not shift the ^4He production rate below the lower error range of $P_{\text{He-4}}$. Significantly higher densities are not expected, as these would imply the presence of a significant share of bedrock-like matrix which is not observed in the sediment core.

The accumulation of ^4He in pore water of sediments can be modelled in terms of production and advective and diffusive transport (Strassmann et al., 2005) by assuming the effective He diffusivity in the pore space to be one order magnitude lower than the molecular diffusivity of He in bulk water (Tomonaga et al., 2011a), the sedimentation rate at Ahlat Ridge to be constant ($0.37 \text{ mm/a} = 220 \text{ m/600 ka}$), and compaction to not reduce the connectivity of pore space. The critical assumption of a single time-independent sedimentation rate is backed by sedimentological investigations showing that the sedimentation rate at Ahlat Ridge is virtually constant over the last 600 ka (Stockhecke et al., 2014a, 2014b). As the sediments of Lake Van consist mainly of clayey silts (i.e., grain sizes of a few tens of microns), the He retention time within the mineral phase can be neglected with regards to the typical time scale of the modelling exercise (i.e., 600 ka).

We used the numerical model of Strassmann et al. (2005), which was specifically developed to simulate the evolution of dissolved (noble) gas concentrations in the pore water of a growing unconsolidated sediment column, to analyse the He dynamics in the sediments of Lake Van. It should be noted that the applied model is not suitable to target specific features within a growing sediment column (i.e., the burial of sediment layers having different production/transport properties cannot be accounted for).

The results of the modelling exercise are shown in Fig. 4 (solid black line). The modelled ^4He concentration profile agrees rather well with the corrected He concentration profile within the uncertainty range given by the He production rate (dashed black lines). This finding suggests that most of the non-atmospheric He in the sediment column is of radiogenic origin and is produced “locally” within the sediment column.

The interpretation that the excess He is produced within the sediments and is of “local” origin is supported by the depth clustering of the measured $^3\text{He}/^4\text{He}$ ratios (Fig. 5). In the depth range between 50 m and 155 m the observed $^3\text{He}/^4\text{He}$ ratios (mean with the respective error: $(2.1 \pm 0.1) \cdot 10^{-6}$) are lower than in the upper section of the sediment column (mean with the respective error: $(2.7 \pm 0.1) \cdot 10^{-6}$). This difference indicates in-situ production of isotopically heavier radiogenic He between 50 and 155 m.

The $^3\text{He}/^4\text{He}$ ratio of the non-atmospheric He in the sediment pore water ($^3\text{He}/^4\text{He}_{\text{ex}}$) is determined by the mixture of the radiogenic He produced in crustal mineral phases ($^3\text{He}/^4\text{He}_{\text{rad}} \approx 2 \cdot 10^{-8}$; e.g., Mamyrin and Tolstikhin, 1984) and He accumulating from a mantle source ($^3\text{He}/^4\text{He}_{\text{mantle}} \approx 10^{-5}$; see Kipfer et al., 1994). If $^3\text{He}/^4\text{He}_{\text{ex}}$ is estimated from the mean $^3\text{He}/^4\text{He}$ ratio of the He excess relative to the ASW concentrations calculated using a temperature of $3.3 \text{ }^\circ\text{C}$ and the measured pore water salinity at the depth of acquisition of each sample ($^3\text{He}/^4\text{He}_{\text{ex}} \approx 2.2 \cdot 10^{-6}$), the linear relationship $^3\text{He}/^4\text{He}_{\text{ex}} = x \cdot ^3\text{He}/^4\text{He}_{\text{mantle}} + (1 - x) \cdot ^3\text{He}/^4\text{He}_{\text{rad}}$ yields $x \approx 0.2$, which indicates that about 20% of the observed non-atmospheric He

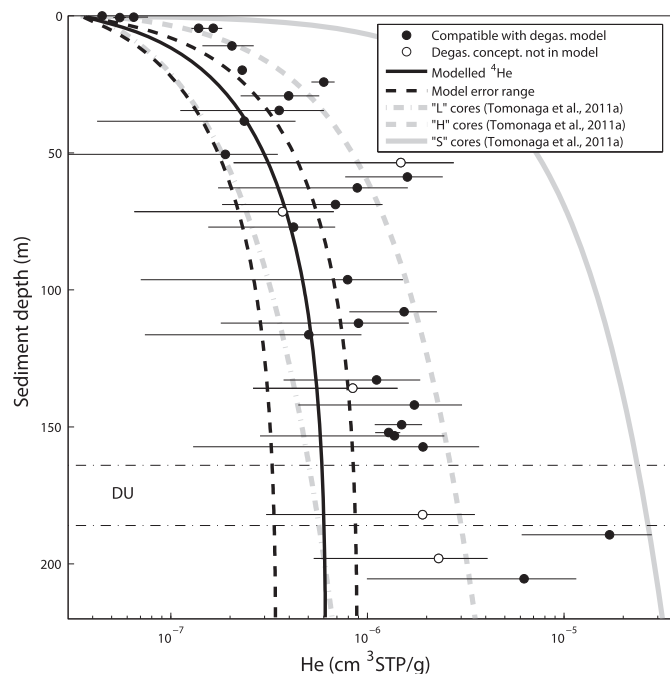


Fig. 4. He concentration profile. Black dots: concentrations corrected for gas loss; empty dots: corrected concentrations for gas loss in samples affected by isotope fractionation. The grey lines represent He concentration gradients determined by a previous study (Tomonaga et al., 2011a): “L” cores (dotted-dashed grey line), “H” cores (dashed grey line), and “S” cores (continuous grey line). The black lines indicate the expected in-situ radiogenic He production (solid black line: mean production rate; dashed black lines: uncertainty of the production rate; see Section 4.2). The horizontal dotted-dashed black lines mark the depth range covered by a deformed unit (DU; see Stockhecke et al., 2014a) characterised by a lower effective diffusivity, as indicated by the sudden change in the He concentration gradient.

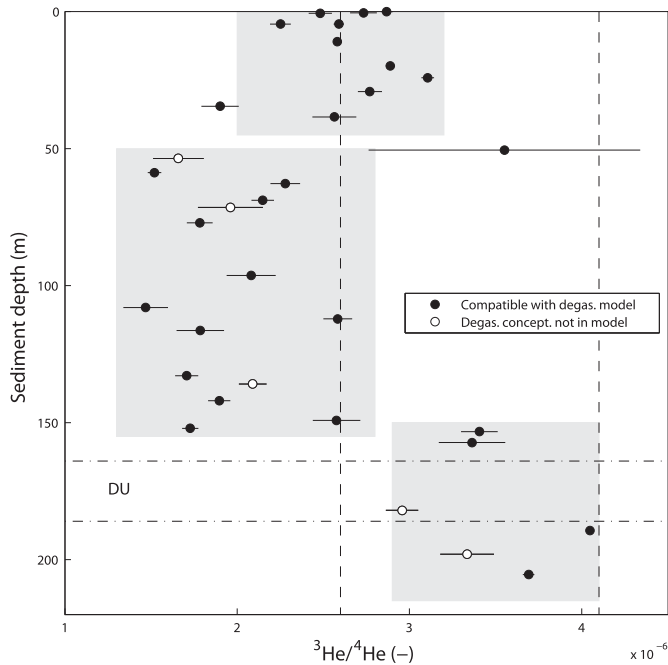


Fig. 5. $^3\text{He}/^4\text{He}$ ratios measured in the ICDP PaleoVan pore water samples. The dashed lines represent the range for the isotope ratios of the terrigenous He emitted into Lake Van (Tomonaga et al., 2011a). The remaining symbols have the same meaning as in Fig. 4. The grey shaded areas are a visual guide to highlight the clustering of the He isotope ratios at different depth ranges (i.e., 0–50 m; 50–155 m; 155–220 m).

surplus is emanating from the deep lithosphere through the sediments at Ahlat Ridge.

In turn, the in-situ radioactive He production in the sediment column accounts for the remaining 80% of the terrigenous He and therefore is identified as the major source of the terrestrial (^4He) He flux through the uppermost 155 m of the sediments of Lake Van. It should be noted that the present estimation of the shares of mantle He and crustal He relies on the assumption that no isotope fractionation occurred during degassing.

In the uppermost 50 m of the sediment column the measured $^3\text{He}/^4\text{He}$ ratios are higher ($(2.7 \pm 0.1) \cdot 10^{-6}$) than between 50 m and 155 m. Below 155 m the observed $^3\text{He}/^4\text{He}$ ratios are even higher ($(3.7 \pm 0.2) \cdot 10^{-6}$) than in the uppermost 50 m. The $^3\text{He}/^4\text{He}$ ratios in the uppermost 50 m and below 150 m depth fall in the range of the typical isotopic signature of terrigenous He emanating into the open water column of Lake Van ($(2.5\text{--}4.1) \cdot 10^{-6}$; Tomonaga et al., 2011a).

Due to the rather homogeneous distribution of U and Th in the sediment column (Baumgarten et al., 2014), we relate the presence of three depth ranges being characterised by different $^3\text{He}/^4\text{He}$ ratios (0–50 m: $(2.7 \pm 0.1) \cdot 10^{-6}$; 50–155 m: $(2.1 \pm 0.1) \cdot 10^{-6}$; 155–220 m: $(3.7 \pm 0.2) \cdot 10^{-6}$) to the specific transport properties of the sediment pore space at Ahlat Ridge (see Section 4.3), and to the dynamics of the terrigenous fluid emission into Lake Van.

The high He isotope ratios in the uppermost 50 m might be the result of lateral fluid transport processes adding a He component enriched in ^3He to the He ascending from the underlying sediments (see Section 4.3).

The increase in the ^3He concentrations with sediment depth implies that the He isotopes diffuse upwards to the sediment–water interface, where they are released into the water body of Lake Van. The isotopic composition of terrigenous He being produced in the deep sediments at Ahlat Ridge between 50 m and 155 m is heavier than the typical terrigenous He accumulating in Lake Van (Tomonaga

et al., 2011a). This suggests that, whereas terrigenous He mainly of radiogenic origin is emitted at Ahlat Ridge, the major release of isotopically light terrigenous He typical for Lake Van has to occur somewhere else within the lake basin.

This conceptual model for the spatial distribution of the He emission into Lake Van is in line with the observation that the strongest He fluxes occur at the steep borders of the main deep Tatvan basin and not in the deepest part of the lake (Fig. 1; Tomonaga et al., 2011a). Our findings are also consistent with the ^3He profiles in the water column (Kipfer et al., 1994; Kaden et al., 2010) that show the highest concentrations not at the sediment–water interface, but some tens of metres above the lake floor.

4.3. Fluid transport properties of the sediment column

The profile of the corrected He concentrations allows characterisation of the fluid transport properties of the sediment column.

The corrected He concentration profile follows the curves of the modelled radiogenic He production and suggests that the effective diffusivity of the sediment column does not change significantly down to approx. 160 m.

A single pore water sample at a depth of 190 m located just below a thick deformed unit (DU, 164–186 m, Fig. 4; Stockhecke et al., 2014a) shows the largest He concentration and the highest measured $^3\text{He}/^4\text{He}$ ratio (Fig. 5). The observed He concentration exceeds the possible concentration range for the in-situ radiogenic He production by far. Both, high concentration and high isotope ratio indicate terrigenous He to accumulate below the DU. The He enrichment suggests that DU acts as a “barrier” constraining He and other fluids/solutes from migrating upwards. The increasing $^3\text{He}/^4\text{He}$ ratios in the lowermost section of the sediment column (>150 m) support the interpretation of a lower permeability within DU as the layer seems to hinder He from the deeper lithosphere from ascending. In turn, such a “barrier” constrains the fluid transport and fosters the accumulation of isotopically light terrigenous He preferentially below DU producing the observed $^3\text{He}/^4\text{He}$ ratio increase with increasing depth. The interpretation that specific sedimentological sequences limit the fluid transport is in line with seismic evidence showing free gases to accumulate or even being “trapped” in event layers (such as DU) in Lake Van (Cukur et al., 2013).

The observation that DU severely constrains the terrestrial fluid emanation at Ahlat Ridge lets us speculate that within and below this unit ancient “palaeo”-water (i.e., water from a past geochemical state of Lake Van) from the time of sediment deposition might be “trapped” and preserved in the pore space (Kwiecien et al., 2012).

In the uppermost 25 m of the sediment core the measured He concentrations are generally higher than the He concentrations predicted by the modelling accounting for the in-situ radiogenic He production and for the vertical solute transport.

This deviation can hardly be attributed to a higher radiogenic He production rate at this depth range exceeding the mean production in the sediments. Baumgarten et al. (2014) report the highest U concentration peak at the Ahlat Ridge drill site at approx. 10 m and elevated U and Th concentrations at a depth of approx. 15 m where the first more than 1-m-thick tephra layer is observed. However, the observation that the $^3\text{He}/^4\text{He}$ ratios in this depth range hardly decrease questions a locally enhanced He production due to higher U and Th activities.

Therefore, the higher He concentrations in the uppermost 25 m seem to point rather to a lateral advective solute transport component affecting the overall emission of terrigenous He. Lateral advective transport of He with an isotope signature similar to the one related to the terrigenous He emission along the steep borders of

the main deep basin of Lake Van (Tomonaga et al., 2011a) may conceptually explain the higher He concentrations and the higher $^3\text{He}/^4\text{He}$ ratios in the uppermost 50 m of the sediment column at Ahlat Ridge.

4.4. Past environmental conditions

Standard regression methods allow to precisely determine the temperature (T) and salinity (S) of the exchanging water mass during the air–water partitioning from the respective dissolved atmospheric noble gas concentrations (Aeschbach-Hertig et al., 1999; Ballentine and Hall, 1999) if the atmospheric pressure (p) prevailing during gas exchange is known (e.g., Kipfer et al., 2002; Brennwald et al., 2004, 2013). These so-called noble-gas temperatures (NGTs) and noble-gas salinities (NGSs) can be calculated by the least-squares fitting of measured noble gas concentrations (Aeschbach-Hertig et al., 1999; Ballentine and Hall, 1999) to the atmospheric noble gas concentrations predicted by Henry's Law (Stute et al., 1995; Aeschbach-Hertig et al., 2000; Kipfer et al., 2002; Aeschbach-Hertig and Solomon, 2013).

As both T and S affect the solubility of noble gases in a similar way, only either NGT or NGS – but not both simultaneously – can be inferred precisely from dissolved noble gas concentrations (Aeschbach-Hertig et al., 1999; Kipfer et al., 2002). In deep cold lakes like Lake Van significant temperature changes are very unlikely to occur in the deep water as internal mixing processes do immediately compensate any large temperature fluctuation and thus the deep-water temperature is always close to the temperature of maximum water density (e.g., Lerman et al., 1995). During the last two decades the temperature at Ahlat Ridge (at a water depth of approximately 350 m) remained almost constant (3.3 ± 0.1 °C; Kaden et al., 2010). We therefore preset T with the deep-water temperature measured at Ahlat Ridge and determined the NGSs from the measured Ne, Ar, Kr and Xe concentrations.

To calculate the NGSs we used Lake Van's specific ASW noble gas concentrations which account for the soda chemistry of the lake water (Tomonaga et al., 2012; see Section 3.2). Due to degassing effects in the deeper core sections, NGSs can only be calculated in a statistically robust manner for samples that are unaffected by gas loss (see Section 4.1 and Fig. 2), i.e., in samples from the uppermost 20 m (corresponding to a sediment age of up to approx. 55 ka; Stockhecke et al., 2014a, 2014b).

The determined NGSs (Fig. 6) increase with increasing depth similarly to the salinity profile measured in the pore water of core catcher samples (although the NGS gradient seems to be steeper than the measured salinity gradient). The highest NGS (42 ± 6 g/kg) occurs at approx. 20 m depth and indicates that the salinity of Lake Van was significantly higher than the present salinity (approx. 23 g/kg; Kempe et al., 1991; Kaden et al., 2010; Tomonaga et al., 2012).

Past major changes in salinity are expected to result in minimum deep-water temperatures ranging from 4 °C (T of maximum water density for $S = 0$ g/kg; i.e., freshwater) to –6 °C (T of maximum water density for $S = 100$ g/kg; i.e., a salinity which is much higher than the pore water salinity measured in Lake Van, Fig. 6). Under the assumption of a higher deep-water temperature of 4 °C, the NGSs would not deviate significantly from those calculated with 3.3 °C. The assumption of a very low deep-water temperature of –6 °C would result in generally higher NGSs (up to 76 ± 2 g/kg at 20 m). Therefore, the NGSs calculated for 3.3 °C are likely to set mainly a lower boundary for the original palaeosalinity and should be considered as rough estimates.

The mean value of the NGS at 20 m being higher than the measured salinity suggests that the latter is not the result of diagenetic processes. A diagenetic salinity increase would imply that the noble-gas concentrations set at the time of deposition are

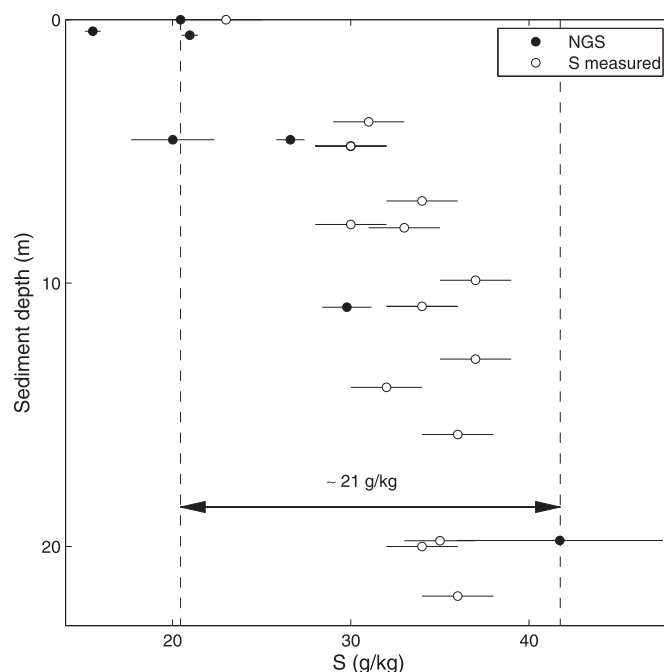


Fig. 6. Salinities measured in the pore water of core catcher samples and noble-gas salinities (NGSs) inferred from the noble-gas concentrations measured in the uppermost 20 m (corresponding to approx. 55 ka BP) of the sediment column of the ICDP PaleoVan cores. The vertical dashed lines are a visual guide indicating the NGSs determined at the sediment/water interface and at 20 m, respectively.

in excess with respect to the new local equilibrium concentrations for higher salinities. Hence calculated NGSs should be lower than the measured salinity – which is in contrast to the observed data.

In terminal lakes such as Lake Van salinity is inversely proportional to the volume of the water body because the total mass of dissolved salts is expected to remain constant over reasonably short time scales. The higher pore water salinity with increasing depth therefore indicates a smaller volume of water and hence a lower lake level in the past. The NGS difference of 21 g/kg (ranging up to 55 g/kg depending on the assumed deep-water temperature) between the pore water at the sediment–water interface and at 20 m depth implies a significantly lower lake level at least 110 m below the present lake level (i.e., not considering the diffusive smoothing of concentration signals over time).

5. Conclusions

This work presents the first attempt to determine not only He, but all noble-gas concentrations in deep-drilling cores of several hundred metres length taken in lacustrine sediments. Until now only very few He, Ne and Ar concentration profiles were analysed in long ocean sediment cores (Barnes and Clarke, 1987; Sano et al., 1992; Torres et al., 1995).

The determined He concentration profile spots the changing transport properties with regards to terrestrial fluid emission in the deep sediments of Lake Van. The He concentrations below 25 m are in agreement with the concentration profile predicted by a model of the in-situ He production and one-dimensional vertical advection/diffusion. The monotonous He concentration increase with increasing depth suggests that fluid transport in the sediments down to approx. 160 m is rather homogeneous. About 80% of terrigenous He in the pore space originates from the in-situ decay of U and Th in the mineral matrix of the sediments. Higher concentrations of He being enriched in ^3He above 25 m imply lateral input of

terrigenous He from the steep borders of the main deep basin towards the sediments in the centre of the lake.

The high He concentration and high $^3\text{He}/^4\text{He}$ ratio at 190 m below a sedimentologically strongly deformed unit (DU) lets us speculate that the DU acts as a less permeable “barrier” limiting the fluid emission.

Palaeosalinities were successfully reconstructed for the uppermost 20 m of the sediment column and indicate that Lake Van had a higher salinity of about 42 ± 6 g/kg during a period of lower lake level.

Acknowledgements

We would like to thank Urs Menet at ETH Zurich for the conception and realisation of the sediment squeezer used for the noble-gas sampling of the ICDP PaleoVan sediment cores. Thanks are also due to two anonymous reviewers for their valuable comments on the manuscript. We thank the PaleoVan team for support during the collection and sharing of data. The PaleoVan drilling campaign was funded by the International Continental Scientific Drilling Program (ICDP), the Deutsche Forschungsgemeinschaft (DFG), the Swiss National Science Foundation (SNF Grants 20FI21_124972, 200021_124981, and 200020_143340) and the Scientific and Technological Research Council of Turkey (Tübitak). The present work was supported by SNF (see the grants mentioned above) and a Marie Curie International Outgoing Fellowship (Contract No. PIOF-GA-2012-332404, Project NoGOS).

References

- Aeschbach-Hertig, W., Peeters, F., Beyerle, U., Kipfer, R., 1999. Interpretation of dissolved atmospheric noble gases in natural waters. *Water Resour. Res.* 35 (9), 2779–2792.
- Aeschbach-Hertig, W., Peeters, F., Beyerle, U., Kipfer, R., 2000. Palaeotemperature reconstruction from noble gases in ground water taking into account equilibration with entrapped air. *Nature* 405, 1040–1044.
- Aeschbach-Hertig, W., Solomon, D.K., 2013. Noble gas thermometry in groundwater hydrology. In: Burnard, P. (Ed.), *The Noble Gases as Geochemical Tracers, Advances in Isotope Geochemistry*. Springer, Berlin, Heidelberg, pp. 81–122.
- Ballentine, C.J., Hall, C.M., 1999. Determining palaeotemperature and other variables by using an error-weighted, nonlinear inversion of noble gas concentrations in water. *Geochim. Cosmochim. Acta* 63 (16), 2315–2336.
- Ballentine, C.J., Burgess, R., Marty, B., 2002. Tracing fluid origin, transport and interaction in the crust. In: Porcelli, D., Ballentine, C., Wieler, R. (Eds.), *Noble gases in Geochemistry and Cosmochemistry, Reviews in Mineralogy and Geochemistry*, vol. 47. Mineralogical Society of America, Geochemical Society, pp. 539–614.
- Barnes, R.O., Clarke, W.B., 1987. Fluid Kinematics, fluid residence times, and rock degassing in oceanic crust determined from noble gas contents of Deep Sea Drilling project pore waters. *J. Geophys. Res.* 92 (B12), 12491–12506.
- Baumgarten, H., Wonik, T., Kwiecien, O., 2014. Facies characterization based on physical properties from downhole logging for the sediment record of Lake Van, Turkey. *Quat. Sci. Rev.* <http://dx.doi.org/10.1016/j.quascirev.2014.03.016> (PaleoVan special issue).
- Berner, R., 1975. Diagenetic models of dissolved species in the interstitial waters of compacting sediments. *Am. J. Sci.* 275, 88–96.
- Beyerle, U., Aeschbach-Hertig, W., Imboden, D.M., Baur, H., Graf, T., Kipfer, R., 2000. A mass spectrometric system for the analysis of noble gases and tritium from water samples. *Environ. Sci. Technol.* 34, 2042–2050.
- Brennwald, M.S., Hofer, M., Peeters, F., Aeschbach-Hertig, W., Strassmann, K., Kipfer, R., Imboden, D.M., 2003. Analysis of dissolved noble gases in the pore water of lacustrine sediments. *Limnol. Oceanogr. Methods* 1, 51–62.
- Brennwald, M.S., Peeters, F., Imboden, D.M., Giral, S., Hofer, M., Livingstone, D.M., Klump, S., Strassmann, K., Kipfer, R., 2004. Atmospheric noble gases in lake sediment pore water as proxies for environmental change. *Geophys. Res. Lett.* 31 (4), L04202.
- Brennwald, M.S., Kipfer, R., Imboden, D.M., 2005. Release of gas bubbles from lake sediment traced by noble gas isotopes in the sediment pore water. *Earth Planet. Sci. Lett.* 235 (1–2), 31–44.
- Brennwald, M.S., Vogel, N., Scheidegger, Y., Tomonaga, Y., Livingstone, D.M., Kipfer, R., 2013. Noble gases as environmental tracers in sediment porewaters and in stalagmite fluid inclusions. In: Burnard, P. (Ed.), *The Noble Gases as Geochemical Tracers, Advances in Isotope Geochemistry*. Springer, Berlin, Heidelberg, pp. 123–153.
- Çağatay, M.N., Ogretmen, N., Damci, E., Stockhecke, M., 2014. Paleoenvironmental records from the northern Basin of Lake Van, Turkey. *Quat. Sci. Rev.* (PaleoVan special issue).
- Chaduteau, C., Fourré, E., Jean-Baptiste, P., Dapoigny, A., Baumier, D., Charlou, J.L., 2007. A new method for quantitative analysis of helium isotopes in sediment pore-waters. *Limnol. Oceanogr. Methods* 5, 425–432.
- Chaduteau, C., Jean-Baptiste, P., Fourré, E., Charlou, J.L., Donval, J.P., 2009. Helium transport in sediment pore fluids of the Congo-Angola margin. *Geochim. Geophys. Geosyst.* 10 (1).
- Craig, H., Lupton, J., 1976. Primordial neon, helium and hydrogen in oceanic basalts. *Earth Planet. Sci. Lett.* 31, 369–385.
- Cukur, D., Krastel, S., Demirel-Schlueter, F., Demirbag, E., Imren, C., Niessen, F., Toker, M., 2012. Sedimentary evolution of Lake Van (Eastern Turkey) reconstructed from high-resolution seismic investigations. *Int. J. Earth Sci.* 102 (2), 571–585.
- Cukur, D., Krastel, S., Schmincke, H.-U., Sumita, M., Çağatay, M.N., Meydan, A.F., Damci, E., Stockhecke, M., 2014a. Seismic stratigraphy of the Lake Van, eastern Turkey. *Quat. Sci. Rev.* <http://dx.doi.org/10.1016/j.quascirev.2014.07.016> (PaleoVan special issue).
- Cukur, D., Krastel, S., Schmincke, H.-U., Sumita, M., Tomonaga, Y., Çağatay, M.N., 2014b. Water level changes in Lake Van, Turkey, during the past ca. 600 ka: climatic, volcanic and tectonic controls. *J. Paleolimnol.* <http://dx.doi.org/10.1007/s10933-014-9788-0>.
- Cukur, D., Krastel, S., Tomonaga, Y., Çağatay, M.N., Meydan, A.F., the PaleoVan science team, 2013. Seismic evidence of shallow gas from Lake Van, eastern Turkey. *Mar. Pet. Geol.* 48, 341–353. <http://dx.doi.org/10.1016/j.marpetgeo.2013.08.017>.
- Imboden, D., 1975. Interstitial transport of solutes in non-steady state accumulating and compacting sediments. *Earth Planet. Sci. Lett.* 27, 221–228.
- Kaden, H., Peeters, F., Lorke, A., Kipfer, R., Tomonaga, Y., Karabiyikoglu, M., 2010. Impact of lake level change on deep-water renewal and oxic conditions in deep saline Lake Van, Turkey. *Water Resour. Res.* 46, W11508.
- Kadioglu, M., Sen, Z., Batur, E., 1997. The greatest soda-water lake in the world and how it is influenced by climate change. *Ann. Geophys.* 15, 1489–1497.
- Kempe, S., Kazermierczak, J., Landmann, G., Konuk, T., Reimer, A., Lipp, A., 1991. Largest known microbialites discovered in Lake Van, Turkey. *Nature* 349, 605–608.
- Keskin, M., 2007. Eastern Anatolia: a hotspot in a collision zone without a mantle plume. *Geol. S. Am. S.* 430, 693–722.
- Kiliñcaşlan, T., 2000. The rising water level in Lake Van: environmental features of the Van basin which increase the destructive effect of the disaster. *Water Sci. Technol.* 42 (1–2), 173–177.
- Kipfer, R., Aeschbach-Hertig, W., Baur, H., Hofer, M., Imboden, D.M., Signer, P., 1994. Injection of mantle type helium into Lake Van (Turkey): the clue for quantifying deep water renewal. *Earth Planet. Sci. Lett.* 125, 357–370. [http://dx.doi.org/10.1016/0012-821X\(94\)90226-7](http://dx.doi.org/10.1016/0012-821X(94)90226-7).
- Kipfer, R., Aeschbach-Hertig, W., Peeters, F., Stute, M., 2002. Noble gases in lakes and ground waters. In: Porcelli, D., Ballentine, C.J., Wieler, R. (Eds.), *Noble gases in Geochemistry and Cosmochemistry, Reviews in Mineralogy and Geochemistry*, vol. 47. Mineralogical Society of America, Geochemical Society, pp. 615–700.
- Kwiecien, O., Tomonaga, Y., Stockhecke, M., Randlett, M.-E., Bucher, S., Pickarski, N., Brennwald, M.S., Schubert, C.J., Kipfer, R., Anselmetti, F.S., Sturm, M., Haug, G.H., 2012. Hydroclimatic changes recorded in Lake Van (eastern Anatolia, Turkey) during the last glacial/interglacial cycle. In: AGU Fall Meeting, San Francisco, United States. Abstract PP41A-2000.
- Kwiecien, O., Stockhecke, M., Pickarski, N., Heumann, G., Litt, T., Sturm, M., Anselmetti, F.S., Kipfer, R., Haug, G., 2014. Dynamics of terminations during the last four glacial terminations recorded in Lake Van, Turkey. *Quat. Sci. Rev.* <http://dx.doi.org/10.1016/j.quascirev.2014.07.001> (PaleoVan special issue).
- Lan, T.F., Sano, Y., Yang, T.F., Takahata, N., Shirai, K., Pinti, D.L., 2010. Evaluating Earth degassing in subduction zones by measuring helium fluxes from the ocean floor. *Earth Planet. Sci. Lett.* 298 (3–4), 317–322.
- Lerman, A., Imboden, D.M., Gat, J.R. (Eds.), 1995. *Physics and Chemistry of Lakes*. Springer, Berlin.
- Litt, T., Krastel, S., Sturm, M., Kipfer, R., Orcen, S., Heumann, G., Franz, S.O., Ulgen, U.B., Niessen, F., 2009. ‘PAEOVAN’, International Continental Scientific Drilling Program (ICDP): site survey results and perspectives. *Quat. Sci. Rev.* 28 (15–16), 1555–1567.
- Litt, T., Anselmetti, F.S., Çağatay, M.N., Kipfer, R., Krastel, S., Schmincke, H.-U., the PaleoVan science team, 2011. A 500,000 year-long sedimentary archive drilled in Eastern Anatolia (Turkey): the PaleoVan Drilling Project. *Eos* 92, 477–479.
- Litt, T., Anselmetti, F.S., Baumgarten, H., Beer, J., Çağatay, M.N., Cukur, D., Damci, E., Glombitza, C., Haug, G.H., Heumann, G., Kallmeyer, J., Kipfer, R., Krastel, S., Kwiecien, O., Meydan, A.F., Orcen, S., Pickarski, N., Randlett, M.-E., Schmincke, H.-U., Schubert, C.J., Sturm, M., Sumita, M., Stockhecke, M., Tomonaga, Y., Vigliotti, L., Wonik, T., the PAEOVAN Scientific Team, 2012. 500,000 Years of Environmental History in Eastern Anatolia: the PAEOVAN Drilling Project. *Scientific Drilling* 14, pp. 18–29.
- Litt, T., Anselmetti, F., 2014. Lake Van deep drilling project PAEOVAN. *Quat. Sci. Rev.* (PaleoVan special issue).
- Litt, T., Pickarski, N., Heumann, G., Stockhecke, M., Polychronis, C.T., 2014. A 600,000 year long continental pollen record from Lake Van, eastern Anatolia (Turkey). *Quat. Sci. Rev.* <http://dx.doi.org/10.1016/j.quascirev.2014.03.017>. PaleoVan special issue, 1–12.
- Mamyrin, B.A., Tolstikhin, I.N., 1984. Helium isotopes in nature. In: *Developments in Geochemistry*, vol. 3. Elsevier, Amsterdam, Oxford, New York, Tokyo.

- O'Nions, R.K., Oxburgh, E.R., 1983. Heat and helium in the Earth. *Nature* 306, 429–431.
- O'Nions, R.K., Oxburgh, E.R., 1988. Helium, volatile fluxes and the development of continental crust. *Earth Planet. Sci. Lett.* 90 (3), 331–347.
- Oxburgh, E.R., O'Nions, R.K., 1987. Helium loss, tectonics, and the terrestrial heat budget. *Science* 237, 1583–1588.
- Ozima, M., Podosek, F.A., 1983. *Noble Gas Geochemistry*. Cambridge Univ. Press, Cambridge, London, New York.
- Randlett, M.-È., Coolen, M.J.L., Stockhecke, M., Pickarski, N., Litt, T., Balkema, C., Kwiecien, O., Tomonaga, Y., Wehrli, B., Schubert, C.J., 2014. Alkenone distribution in Lake Van sediments since the last 270 ka: influence of temperature and haptophyte species composition. *Quat. Sci. Rev.* <http://dx.doi.org/10.1016/j.quascirev.2014.07.009> (PaleoVan special issue).
- Sano, Y., Sakamoto, M., Ishibashi, J., Wakita, H., Matsumoto, R., 1992. Helium isotope ratios of pore gases in deep-sea sediments, leg 128. In: Pisciotta, K.A., Ingle, J.C., von Breymann, M.T., Barron, J. (Eds.), *Proc. ODP, Scient. Res.* 127/128, pp. 747–751.
- Schlosser, P., Winckler, G., 2002. Noble gases in ocean waters and sediments. In: Porcelli, D., Ballentine, C., Wieler, R. (Eds.), *Noble gases in Geochemistry and Cosmochemistry, Reviews in Mineralogy and Geochemistry*, vol. 47. Mineralogical Society of America, Geochemical Society, pp. 701–730.
- Stanley, R.H.R., Jenkins, W.J., 2013. Noble gases in seawater as tracers for physical and biogeochemical ocean processes. In: Burnard, P. (Ed.), *The Noble Gases as Geochemical Tracers, Advances in Isotope Geochemistry*. Springer, Berlin, Heidelberg, pp. 55–79.
- Stockhecke, M., Sturm, M., Brunner, I., Schmincke, H.-U., Sumita, M., Kipfer, R., Kukur, D., Kwiecien, O., Anselmetti, F.S., 2014a. Sedimentary evolution and environmental history of Lake Van (Turkey) over the past 600,000 years. *Sedimentology*. <http://dx.doi.org/10.1111/sed.12118>.
- Stockhecke, M., Kwiecien, O., Vigliotti, L., Anselmetti, F.S., Beer, J., Çağatay, M.N., Channell, J.E.T., Kipfer, R., Lachner, J., Litt, T., Pickarski, N., Sturm, M., 2014b. Chronostratigraphy of the 600,000 year old continental record of Lake Van (Turkey). *Quat. Sci. Rev.* <http://dx.doi.org/10.1016/j.quascirev.2014.04.008> (PaleoVan special issue).
- Strassmann, K., Brennwald, M.S., Peeters, F., Kipfer, R., 2005. Dissolved noble gases in porewater of lacustrine sediments as palaeolimnological proxies. *Geochim. Cosmochim. Acta* 69 (7), 1665–1674.
- Stute, M., Forster, M., Frischkorn, H., Serejo, A., Clark, J.F., Schlosser, P., Broecker, W.S., Bonani, G., 1995. Cooling of tropical Brazil (5‰) during the Last Glacial Maximum. *Science* 269, 379–383.
- Sumita, M., Schmincke, H.-U., 2013a. Impact of volcanism on the evolution of Lake Van I: evolution of explosive volcanism of Nemrut Volcano (eastern Anatolia) during the past >400,000 years. *Bull. Volcanol.* 75 (5), 1–32.
- Sumita, M., Schmincke, H.-U., 2013b. Impact of volcanism on the evolution of Lake Van II: temporal evolution of explosive volcanism of Nemrut Volcano (eastern Anatolia) during the past ca. 0.4 Ma. *J. Volcanol. Geotherm. Res.* 253, 15–34.
- Tomonaga, Y., Brennwald, M.S., Kipfer, R., 2011a. Spatial distribution and flux of terrigenous He dissolved in the sediment pore water of Lake Van (Turkey). *Geochim. Cosmochim. Acta* 75 (10), 2848–2864. <http://dx.doi.org/10.1016/j.gca.2011.02.038>.
- Tomonaga, Y., Brennwald, M.S., Kipfer, R., 2011b. An improved method for the analysis of dissolved noble gases in the pore water of unconsolidated sediments. *Limnol. Oceanogr. Methods* 9, 42–49. <http://dx.doi.org/10.4319/lom.2011.9.42>.
- Tomonaga, Y., Blättler, R., Brennwald, M.S., Kipfer, R., 2012. Interpreting noble-gas concentrations as proxies for salinity and temperature in the world's largest soda lake (Lake Van, Turkey). *J. Asian Earth Sci.* 59, 99–107. <http://dx.doi.org/10.1016/j.jseaes.2012.05.011>.
- Tomonaga, Y., Brennwald, M.S., Kipfer, R., 2013. Using helium and other noble gases in ocean sediments to characterize active methane seepage off the coast of New Zealand. *Mar. Geol.* 344, 34–40. <http://dx.doi.org/10.1016/j.margeo.2013.07.010>.
- Torres, M., Bayer, R., Winckler, G., Suckow, A., Froelich, P., 1995. Elemental and isotopic abundance of noble gases in formation fluids recovered in situ from the Chile Triple Junction. In: Lewis, S., Behrmann, J., Musgrave, R., Cande, S. (Eds.), *Proceedings of the Ocean Drilling Program, Scientific Results*, vol. 141. ODP, College Station TX, pp. 321–329.
- Tyroller, L., Brennwald, M.S., Mächler, L., Livingstone, D.M., Kipfer, R., 2014. Fractionation of Ne and Ar isotopes by molecular diffusion in water. *Geochim. Cosmochim. Acta* 136, 60–66. <http://dx.doi.org/10.1016/j.gca.2014.03.040>.
- Vigliotti, L., Channell, J.E.T., Stockhecke, M., 2014. Paleomagnetic and rock magnetic studies from Lake Van sediments: implications for chronology and paleo-environment since 350 ka. *Quat. Sci. Rev.* (PaleoVan special issue).
- Zartman, R.E., Wasserburg, G.J., Reynolds, J.H., 1961. Helium, argon, and carbon in some natural gases. *J. Geophys. Res.* 66 (1), 277–306.